Synthesis of coordination polymers of tetravalent actinides (U and Np) with phthalate or mellitate ligand in aqueous medium

Martin, N. P.; März, J.; Volkringer, C.; Henry, N.; Hennig, C.; Ikeda-Ohno, A.; Loiseau, T.;

Originally published:

February 2017

Inorganic Chemistry 56(2017)5, 2902-2913

DOI: https://doi.org/10.1021/acs.inorgchem.6b02962

Perma-Link to Publication Repository of HZDR:

https://www.hzdr.de/publications/Publ-24379

Synthesis of coordination polymers of tetravalent actinides (U and Np) with phthalate or mellitate ligand in aqueous medium.

Nicolas P. Martin,[a] Juliane März,[b] Christophe Volkringer,[a,c] Natacha Henry,[a] Christoph Hennig,[b] Atsushi Ikeda-Ohno[b] and Thierry Loiseau.[a,*]

[a]*Unité de Catalyse et Chimie du Solide (UCCS) – UMR CNRS 8181, Université de Lille, ENSCL, Bat C7, BP 90108, 59652 Villeneuve d'Ascq, France.*
[b]*Helmholtz-Zentrum Dresden-Rossendorf, Institute of Resource Ecology, Bautzner Landstrasee 400, 01328 Dresden, Germany.*
[c]*Institut Universitaire de France (IUF), 1, rue Descartes, 75231 Paris cedex 05, France.*

[*] To whom correspondence should be addressed. E-mail: thierry.loiseau@ensc-lille.fr. Phone: (33) 3 20 434 122, Fax: (33) 3 20 43 48 95.

To be submitted to Inorg. Chem.
Version december 5, 2016

Abstract: Four coordination polymers bearing uranium or neptunium have been hydrothermally synthesized at 130°C, from a tetravalent actinide chloride ($AnCl_4$) source in association with phthalic (noted 1,2-H_2bdc hereafter) or mellitic (noted H_6mel hereafter) acid in aqueous media. With the phthalate ligand, two analogous assemblies ($[An_2O_2(H_2O)_2(1,2\text{-}bdc)_2]\cdot H_2O$; An = U^{4+} (**1**) or Np^{4+} (**2**)) have been isolated and are built up from the connection of square anti-prismatic polyhedra (AnO_8) linked to each other via μ_3-oxo groups (edge-sharing mode) forming infinite zig-zag ribbons. The phthalate molecules connect adjacent chains to each other generating a 2D network. Water molecules are bonded to the actinide center or found intercalated between the layers. With the mellitate ligand, two distinct structures have been identified. The uranium-based compound ($U_2(OH)_2(H_2O)_2$(mel) (**3**)) exhibits a 3D structure composed of dinuclear units of UO_8 polyhedra (square anti-prism) linked via common edge (μ_2-hydroxo). Mellitate linkers connect with a part of its six carboxylate arms the dinuclear bricks to a 3D framework. The structure of the neptunium mellitate ($[(NpO_2)_{10}(H_2O)_{14}(Hmel)_2]\cdot 12H_2O$ (**4**)) reveals the oxidation of the initial Np(IV) toward Np(V) in our synthetic hydrothermal conditions, and this generates typical neptunyl entities with pentagonal bipyramidal environment (NpO_7 unit). The resulting network is a layered assembly, composed of sheets of NpO_7 linked in a square net, with cation-cation interactions between neptunyl bond (Np=O) and Np-O bonds from the pentagonal plane. The cohesion of the 3D structure is caused by the mellitate molecules acting as bridging linkers between the NpO_7 sub-network. For the mellitate, only four carboxylate groups are involved in the connection of the NpO_7-based layer.

Keywords: coordination polymer, uranium, neptunium, phthalic acid, mellitic acid, crystal structure.

Introduction

The research of coordination polymers bearing actinides have grown exponentially in the last decades, owing to the development of the metal-organic frameworks (MOF) class, mainly based on the combination of metallic centers with O- or N-donor organic ligands (typically carboxylate) leading to three-dimensional porous architectures. In the series of actinides (An), uranium would be of the major importance in general. It is a naturally occurring element and is stabilized under oxic conditions as a hexavalent state in the form of the uranyl cation, UO_2^{2+}, with two trans-oxo U=O bonds, whereas the tetravalent uranium occurs under anoxic conditions as U^{4+} ion. The uranyl(VI) moiety is able to react with a large number of organic carboxylic acids in order to generate a wide variety of mixed uranyl-organic frameworks (UOF) with different dimensionalities (from 0D to 3D) and bearing mono or polynuclear inorganic uranyl-centered sub-units.[1-3]

As compared with a considerable amount of investigations on the UOF, the studies on the actinides with other oxidation states, as for instance +4, interacting with this type of polycarboxylic acids are scarce even to date and the precedent works have dealt mainly with

Th(IV) and U(IV) complexes. For these two An elements, most of the studies have reported the syntheses and descriptions of networks with different nuclearities of An(IV) building units. A typical illustration of such polynuclear brick is the hexanuclear cationic core $[An_6O_4(OH)_4]^{12+}$, which has been stabilized by many carboxylate ligands, with Th,[4-9] U[4,10-14] and Pu,[15,16] as crystalline products. Similar hexameric bricks are also observed with Ce(IV),[17-21] which can be used as surrogate element for actinide. Most of these works has described the association of aromatic poly-carboxylate ligands (for example, benzoates, terephathalates, trimesates, …) with such light actinides in the complex assemblies or polymer coordination type, which were synthesized by using commonly diffusion/slow evaporation or solvothermal route with organic solvent (DMF, THF…).[9,10,13,14,22-36] There are, however, only a few studies using pure aqueous reaction media which would be more relevant to the environmental conditions.[37] In this case, the use of O- or N-donor organic ligands may favor the isolation of discrete polynuclear entities bearing An(IV),[4-8] which easily undergo hydrolysis and condensation reactions in aqueous solution.[37,38] Therefore, the knowledge of the evolution of such aqueous An(IV) species would be of potential importance for the understanding of the migration of An in the geosphere.[39]

Although precedent literature have described many examples of An(IV) coordination polymers obtained in organic solvent media, only a few reports has explored the reactivity of such 5f cationic species (or just cations) with polydentate carboxylic acids in aqueous solutions. For instance, the formation of An(IV) oxalates have been extensively investigated due to its importance in the spent nuclear fuel reprocessing by PUREX.[40] More recently, the reaction of Th(IV) with trimesic acid has been reported in aqueous medium.[26] The reactions of with phthalate ligands with U(IV), have been investigated, resulting in the formation of a dinuclear complex under bio-relevant anaerobic conditions in the presence of bacteria.[41] This bidentate carboxylate aromatic molecule can be often found in the environment, mainly derived from the natural decomposition of humic and fulvic acids.

Based on these backgrounds, the aim of this study is to investigate the reaction of such phthalate ligands with U(IV) under aqueous conditions. The work is further extended to the use of mellitate (1,2,3,4,5,6-benzenehexacarboxylate), which also can be found in natural soils, especially in natural mineral aluminum salts.[42] Since similar issues of soil contamination is related with the geological disposal of radioactive wastes,[43,44] the study is also extended to neptunium (Np), which is a parent nuclide of U. In fact, the crystal chemistry of Np(IV) is poorly investigated even to date. To the best of your knowledge, only two publications have described the crystalline formation of Np(IV) carboxylates. Both contributions gave descriptions of Np(IV) monocarboxylates of formate (as $Np(HCOO)_4$[45]) and the tribromoacetate (as $Np(CBr_3COO)_4$[46]), obtained from a precipitation method. This situation is in contrast with those of other oxidation states of Np, reporting many carboxylate coordination complexes or polymers for Np(V)[47-62] and Np(VI).[63-67]

The present study describes the hydrothermal syntheses and crystal structures of U(IV) and Np(IV) phthalates ($[An_2O_2(H_2O)_2(1,2\text{-bdc})_2]\cdot H_2O$ (An = U^{4+} (**1**), Np^{4+} (**2**)), as well as the U(IV) mellitate $U_2(OH)_2(H_2O)_2(mel)$ (**3**). In our synthesis conditions, a distinct compound ($[(NpO_2)_{10}(H_2O)_{14}(Hmel)_2]\cdot 12H_2O$ (**4**)) containing Np(V) has been isolated in the presence of mellitic acid, whereas the isostructural Np(IV) phase of the U(IV) complex was not produced.

We also report the thermal behavior and optical properties (infrared and UV-Vis) of the U(IV) phthalate, which has been obtained as pure phase.

Experimental section

Synthesis. ***Caution!*** *Natural U and ^{237}Np are radioactive and chemically toxic reactants. Therefore, precautions with suitable equipments and facility for radiation protection are required for handling these elements. Experiment with ^{237}Np was carried out in a controlled laboratory at the Institute of Resource Ecology (Helmholtz-Zentrum Dresden-Rossendorf, Germany), which possesses appropriate equipments for handling highly radioactive elements.* The compounds have been hydrothermally synthesized under autogenous pressure using 2 mL glass vial with Teflon cap by using the following chemical reactants: uranium tetrachloride (UCl_4, obtained according to the protocol using the reaction of hexachloropropene with uranium oxide UO_3[25]), neptunium tetrachloride ($NpCl_4$, obtained from a similar protocol using the reaction of hexachloropropene with neptunium oxide $^{237}NpO_2$, from ≈50 mg sample), phthalic acid ($C_8H_6O_4$, 1,2-H_2bdc, Acros Organics, 99%), mellitic acid ($C_{12}H_6O_{12}$, H_6mel, Aldrich, 99%) and deoxygenated de-ionized water. The chemicals (except UCl_4 and $NpCl_4$) are commercially available and have been used without any further purification. The preparation of reactant mixtures with UCl_4 and $NpCl_4$ were performed in an inert gas glove box under argon (Lille) or nitrogen (Dresden) atmosphere. The mixtures were then transferred into closed glass vials, removed from the glove box and then heated in an oven under ambient atmosphere.

$[U_2O_2(H_2O)_2(1,2\text{-bdc})_2]\cdot H_2O$ (**1**): a mixture of 12 mg (0.03 mmol) UCl_4, 23 mg (0.14 mmol) phthalic and 0.5 mL (27.8 mmol) H_2O was placed in a closed glass vial and then heated statically at 130°C for 24 hours. The resulting product of **1** (green flat needle-like crystallites – Figure S1a) was then filtered off, washed with N,N-dimethyformamide (DMF) and dried at room temperature under ambient atmosphere. Scanning electron microscopy shows the formation of flat needle-shape crystallites (Figure S1a). Compound **1** was obtained as a pure phase, which is proved by the obtained powder X-ray diffraction pattern, being compared to the simulated one (Figure S2a).
$[Np_2O_2(H_2O)_2(1,2\text{-bdc})_2]\cdot H_2O$ (**2**): a mixture of 12 mg (0.03 mmol) $NpCl_4$, 23 mg (0.14 mmol) phthalic acid and 0.5 mL (27.8 mmol) H_2O was placed in a closed glass vial and then heated statically at 130°C for 24 hours. The resulting product of **2** (brown flat needle-like crystallites – Figure S1c) was dried at room temperature under ambient atmosphere. Powder XRD analysis (Figure S2c) as well as optical microscope show that some unidentified impurities are present together with the phase **2**.
$U_2(OH)_2(H_2O)_2$(mel) (**3**): a mixture of 12 mg (0.03 mmol) UCl_4, 40 mg (0.12 mmol) mellitic acid, 50 μL (0.2 mmol) NaOH (4M) and 1 mL (55.5 mmol) H_2O was placed in a closed glass vial and then heated statically at 130°C for 24 hours. The resulting product of **3** (green plate-like crystallites – Figure S1b) was then filtered off, washed with water and dried at room temperature under ambient atmosphere. The examination of the powder XRD pattern (Figure

S2b) indicates that the compound **3** is not observed as pure phase and an unidentified compound is always obtained with **3**.
$[(NpO_2)_{10}(H_2O)_{14}(Hmel)_2]\cdot 12H_2O$ (**4**): a mixture of 10 mg (0.026 mmol) $NpCl_4$, 40 mg (0.12 mmol) mellitic acid, 50 μL (0.2 mmol) NaOH (4M) and 1 mL (55.5 mmol) H_2O was placed in a closed glass vial and then heated statically at 130°C for 24 hours. The resulting product of **4** (green platelet-like crystallites – Figure S1d) was dried at room temperature under ambient atmosphere. Powder XRD analysis (Figure S2d) as well as optical microscope show that some unidentified impurities are present together with the phase **4**.

Single-crystal X-ray diffraction. Crystals of the uranium compounds (**1** and **3**) were analyzed on a Bruker DUO-APEX2 CCD area-detector diffractometer at 300K, using microfocused Mo-K_α radiation (λ = 0.71073 Å) with an optical fiber as collimator (at UCCS, University of Lille). Crystals of the neptunium compounds (**2** and **4**) were analyzed on a Bruker D8 VENTURE diffractometer with a PHOTON 100 CMOS detector at 100K, using microfocus Mo-K_α radiation (λ = 0.71073 Å) (at Helmholtz-Zentrum Dresden-Rossendorf). Crystals of **1**-**4** were selected under polarizing optical microscope and glued on a glass fiber for a single-crystal X-ray diffraction experiments. Several sets of narrow data frames (20 s per frame) were collected at different values of θ for two initial values of ϕ and ω, respectively, using 0.3° increments of ϕ or ω. Data reduction was accomplished using SAINT V7.53a.[68] The substantial redundancy in data allowed a semi-empirical absorption correction (SADABS V2.10[69]) to be applied, on the basis of multiple measurements of equivalent reflections. The structure was solved by direct methods, developed by successive difference Fourier syntheses, and refined by full-matrix least-squares on all F^2 data using SHELX[70] program suite. Hydrogen atoms of the benzene ring were included in calculated positions and allowed to ride on their parent atoms. The final refinements include anisotropic thermal parameters of all non-hydrogen atoms, except the oxygen atoms of the water molecules. Crystals of compound **4** were systematically twinned and the issue twining treatment was performed by using JANA[71] software. Afterward refinements indicate 57% of domain I and consequently 43% of domain II, with the orientation matrix -0.0011 -1.0011 -0.1396; -0.9989 0.0011 0.1396; 0 0 -1. The crystal data are given in Table 1. Supporting information is available in CIF format. CCDC file numbers: 1509604-1509607.

Powder X-ray diffraction. The powder X-ray diffraction patterns (compounds **1** and **3**) were collected at room temperature with a D8 advance A25 Bruker apparatus with Bragg–Brentano geometry (θ-2θ mode). The D8 diffractometer is equipped with a LynxEye detector with CuKα radiation. For compounds **2** and **4**, powder X-ray patterns have been collected on a Rigaku MiniFlex 600 (θ-2θ mode, CuKα source with 40 kV / 15 mA for X-ray generation), equipped with a D/Tex Ultra Si strip detector with a standard detection mode.

X-ray thermodiffraction. X-ray thermodiffractometry was performed for compound **1** under 5 $L.h^{-1}$ nitrogen flow in an Anton Paar HTK1200N of a D8 Advance Bruker diffractometer (θ-θ mode, CuKα radiation) equipped with a Vantec1 linear position sensitive detector (PSD). Each powder pattern was recorded in the range 5-50° (2θ) (at intervals of 20°C between RT

and 800°C) with a 1s/step scan, corresponding to an approximate duration of 37 min. The temperature ramps between two patterns were 5°C.min^{-1}.

Thermogravimetric analysis. The thermogravimetric experiment was carried out on a thermo-analyzer TGA 92 SETARAM under argon atmosphere with a heating rate of 5°C.min^{-1} from room temperature up to 1100°C.

Infrared spectroscopy. Infrared spectra of compounds **1** and **3** (see Supplementary Information) were measured on Perkin Elmer Spectrum Two^{TM} spectrometer between 4000 and 400 cm^{-1}, equipped with a diamond Attenuated Total Reflectance (ATR) accessory. Phase transformation of compound **1** was characterized by in situ IR spectroscopy in air with a heating rate of 10°C.min^{-1} from RT up to 210°C. During this period, 195 spectra were recorded in the range 4000–400 cm^{-1}, with a resolution of 4 cm^{-1}, on a Perkin–Elmer Spectrum Two spectrometer, equipped with a Pike Special-IR GladiATR accessory.

UV/Visible spectroscopy. UV/Vis spectra have been collected by using a Perkin-Elmer Lambda 650 spectrophotometer equipped with a powder sample holder set.

Results

Structure description

The association of tetravalent U(IV) or Np(IV) cation with the phthalate molecule resulted in the formation of an identical coordination polymer network $[An_2O_2(H_2O)_2(1,2\text{-bdc})_2]\cdot H_2O$ (An = U^{4+} (**1**), Np^{4+} (**2**)), which possesses a 2D organic-inorganic assembly. Their crystal structure is based on two crystallographically independent An centers (Figure 1), which exhibit the same coordination geometry: the metals An1 and An2 are eight-fold coordinated by three oxo groups (O1, O2), four carboxyl oxygen atoms (labeled O_C, from phthalate molecule) and one aquo species (O1W, O2W). It defines a distorted square anti-prismatic geometry (AnO_8), with typical U-O bond lengths of 2.178(4)-2.376(4) Å, U-OW bond distances of 2.616(5)-2.626(4) Å and U-O_C bond distances in the range 2.329(4)-2.483(4) Å. Due to the actinide contraction,[72] the corresponding Np-O bond distances are slightly shorter than the corresponding U-O distances, with Np-O bond distances of 2.185(3)-2.362(3) Å, Np-OW bond distances of 2.617(3)-2.625(3) Å and Np-O_C bond distances in the range 2.338(3)-2.484(3) Å. Indeed, the oxo groups are shared between three adjacent actinide centers, with a μ_3 bridging configuration, whereas the aquo species are in a terminal position. The assignment of μ_3-O/H_2O groups are in good agreement with bond valence calculations,[73] which give the values of 2.03 and 2.11 for O1 and O2 in the uranium-based compound (expected value: 2.0). For the aquo species, bond valence calculations give 0.26 and 0.25 for O1W and O2W in the uranium-based compound (expected value: 0.4). The existence of the μ_3-O bridging groups leads to the formation of an infinite ribbon, with AnO_8 units sharing two edges with adjacent one (Figure 2). Within this chain, the interatomic U···U distances are

3.6645(4) and 3.7094(5) Å, for U1···U2 and U1···U1, respectively. In the neptunium analog, the Np···Np distances are 3.6438(4) and 3.7031(5) Å, for Np1···Np2 and Np1···Np1, respectively. For comparison, U···U distances are slightly longer, with the values of 3.866(1) Å in UO_2[74] and 3.842(1) Å in NpO_2[75] fluorite structures, respectively. The occurrence of such infinite one-dimensional network is not so common in coordination polymers with An(IV) and discrete monomeric or polynuclear complexes are usually observed instead. In fact, a closely related chain has been previously described in the U(IV)-containing network $[U_2O_2(bdc)_2(DMF)]$[14] involving the terephtalate (bdc) linker. A second type of infinite extended chain occurs with acetate ligands,[76] but the connection of the bicapped square antisprimatic polyhedra (UO_{10}) via a trans edge-sharing mode, generates straight ribbons instead of the zig-zag one found in the compounds **1**-**2**. A cis edge-sharing connection mode was encountered in the uranium sulfate $U(OH)_2(SO_4)$,[77] in which uranium is eight-fold coordinated in square antiprismatic geometry). Within one inorganic chain, aligned along the *a* axis, there is one type of phthalate molecules bridging two pairs of An1-O-An2 sub-units; each carboxylate arm adopt a *syn-syn* configuration in a bidentate bridging mode between the An1 and An2 centers (Figure 2). A second type of phthalate molecules plays the role of linkers between two adjacent chains, with the same *syn-syn* bidentate connection fashion. This mode generates the formation of organic-inorganic layers $[An_2O_2(H_2O)_2(1,2\text{-bdc})_2]$ in the (*a*,*b*) plane (Figure 3). Free water molecules (OW3) are intercalated between the hybrid sheets stacking along the *c* axis. The O3W species reveals strong hydrogen bond interactions with the attached water molecule O2W (O3W···H2WA-O2W = 2.088(10) Å in **1**; O3W···H2WA-O2W = 2.016(6) Å in **2**). The cohesion of the structure is caused via the van der Waals interaction between the benzene rings. However, based on thermogravimetric analysis, the water content of the uranium compound was determined to be $0.5H_2O$ (per U_2O_2 unit), instead of $1H_2O$ (per U_2O_2 unit) revealed by XRD (see thermal behavior section). This difference might reflect a disorder with a partial occupancy for the free water molecules of O3W type. The solid-state UV-visible absorption spectrum (Figure S3d) has been collected at room temperature for the compound **1** and is typical for U(IV) with f-f transitions.[78] It consists of a broad band between 600 and 700 nm, with some resolved components at 629, 654 and 678 nm (assigned to the transitions $^3H_4 \rightarrow {}^1G_6$ $^3H_4 \rightarrow {}^1D_2$ and $^3H_4 \rightarrow {}^3P_0$). Two other peaks at 500 and 550 nm also observed and could be related to the transitions $^3H_4 \rightarrow {}^1I_6$ and $^3H_4 \rightarrow {}^3P_1$, respectively.

The crystal structure of compound **3** ($U_2(OH)_2(H_2O)_2(mel)$) consists of one crystallographically independent U(IV) cation coordinated with five carboxyl oxygen (O_C) atoms, two hydroxo (OH) and aquo (O1W) groups (Figure 4). The U-O bond distances are ranging from 2.288(18) up to 2.430(18) Å for O_C. The U1-OH bond lengths are 2.255(17) and 2.376(14) Å, whereas the U1-O1W is slightly longer with bond distance of 2.52(2) Å. The assignments of the OH/OH_2 are in good agreement from the bond valence calculations,[73] with the values of 1.18 for O1OH (expected value for OH group: 1.2) and 0.33 for the O1W (expected value for H_2O: 0.4). The eight-fold coordinated uranium U1 is defined by a square antiprismatic polyhedron, which is linked via a common edge to an adjacent uranium center around a 2 axis operation (U1···U1 distance = 3.775(2) Å). The corresponding bridging group is the μ_2-OH species. The aquo ligand is in terminal position in the coordination sphere of U1,

and is not further linked to another uranium atom. The resulting dinuclear unit $\{U_2O_{10}(OH)_2(H_2O)_2\}$ is connected to each other through the mellitate molecules. The latter adopts an eight-fold coordination with the uranium centers (Figure 4). Two of its carboxylate arms exhibit a *syn-syn* bidentate bridging fashion with the uranium centers; two others have a *syn-anti* bidendate bridging mode; the last two carboxylate groups adopt an *anti*-monodentate connection mode. For the latter, the remaining non-bonded C-O distance is 1.20(4) Å (C6-O62) and related to a C=O bonding. When viewing down the [001] direction (Figure 5), the crystal structure shows a layer of dinuclear uranium-centered units linked to each other via the mellitate molecules with the *anti*-monodentate and the *syn-anti* bidendate carboxylate arms. The other carboxylate groups of mellitate ligand ensure the connection of the uranium atoms along the [011] direction, in order to generate a rather dense three-dimensional coordination polymer network (Figure 5). The formation of such dinuclear entity with a double μ_2-OH bridge is quite unique in the chemistry of U(IV) compounds.[37] Up to now, only one literature has reported the formation of dinucelar U(IV) organometallic complex, involving the chelating ligand 1,2,3,4-tetramethyl-5-(2-pyridil)cyclopentadiene.[79] In the latter species, the two uranium centers are bridged by two μ_2-oxo groups, not by μ_2-OH ones.

The structural analysis of compound **4** reveals that the hydrothermal reaction of $NpCl_4$ with the mellitic acid results in an unexpected Np(V)-based network although neptunium exists as Np(IV) in the compound **2** with the phthalate molecule. Indeed, one Np(V) mellitate complexe ($Na_4(NpO_2)_2(mel)\cdot 8H_2O$[58]) has already been described with sodium as counter-cationic species, from slow evaporation process of an aqueous solution at pH = 6.5. In our hydrothermal conditions, a distinct structural assembly $[(NpO_2)_{10}(H_2O)_{14}(Hmel)_2]\cdot 12H_2O)$ has been produced. It consists of ten crystallographically independent neptunium atoms with seven-fold coordinations (pentagonal bipyramids). Typical double *transdioxo* neptunyl bonds are observed for all the cations. The Np=O bond lengths are ranging from 1.824(8) up to 1.872(7) Å. The Np-O bonding lengths associated with carboxyl oxygen in the equatorial pentagonal plane, are ranging from 2.342(7) up to 2.653(7) Å. The formation of terminal Np-O bonds is also observed, where oxygen atoms have been assigned to aquo species. The Np-OH_2 bond lengths are in the range 2.448(7)-2.566(7) Å. These values have been observed in the other Np(V) compounds, with similar coordination environments.[51,61,80-83] However, the coordination sphere of the different neptunium centers can be distinguished by the presence or not, of terminal aquo groups. Indeed, only Np7 contains three carboxyl oxygen atoms in the equatorial plane ($\{NpO_7\}$ unit). One terminal aquo species is observed for Np2, Np4, Np8 and Np9 ($\{NpO_6(H_2O)\}$ unit), whereas two terminal aquo ligands are present in the coordination sphere of Np1, Np3, Np5, Np6 and Np10 ($\{NpO_5(H_2O)_2\}$ unit; Figure 6). All the neptunium atoms are linked to each other via their two 'yl' oxo groups, which correspond to the oxo groups in the equatorial pentagonal plane of the adjacent metallic cations. The linkage of Np=O-Np type is not surprising for Np(V) and it has been reported as cation-cation interaction (CCI) in many Np-based compounds.[84] The corresponding Np-O bond lengths are varying from 2.385(7) up to 2.509(7) Å in the equatorial plane. The resulting CCI connection mode of the neptunium centers via their two transdioxo double 'yl' oxo group generates a two-dimensional inorganic square network (Figure 7), developing in the pseudo-tetragonal (*a*,*b*) plane (indeed, *a* and *b* cell parameters are very close, with values of 12.9650(3) and 12.9796(3) Å, respectively). The Np···Np distances between neighboring neptunium centers

are in the range 3.937(1)-4.261(1) Å. In fact, this layer is related to that observed in the neptunium phthalate $[(NpO_2)_2(1,2\text{-bdc})]\cdot 4H_2O$[61] or isophthalate $[(NpO_2)_2(1,3\text{-bdc})(H_2O)]\cdot H_2O$[51] obtained by using the hydrothermal route, from a nitrate neptunium(V) source $NpO_2(NO_3)$. Similar square net-like sheets have been encountered in inorganic compounds (sulfates, selenates, borates, iodates, …).[80,81,85-88] The resulting square net is linked to each other through the hexatopic mellitate molecules. Two types of crystallographically independent organic linkers (labeled A and B) are observed in the structure of **4** (Figure 8). Both mellitate molecules adopt a seven-fold coordination state with the neptunium atoms. Two of the carboxylate arms exhibit a *syn-syn* bidentate bridging mode with Np centers (with Np2, Np3 and Np4, Np2 for A; with Np1, Np6 and Np4, Np5 for B). One other carboxylate arm adopts a *syn-anti* bidenate bridging fashion (with Np8, Np10 for A; with Np8, Np7 for B). A fourth carboxylate arm is chelating one Np center (Np9 for A; Np7 for B). The two remaining carboxylate groups are not bound to the neptunium centers: one exists in its protonated form with an elongated C-OH bondings (1.289(12) and 1.318(12) Å in A, and B, respectively) and short C=O bondings, (1.222(12) and 1.210(12) Å in A, and B, respectively); the second non-bonded carboxylate group is not protonated with C-O bond distance, varying from 1.229(11) up to 1.245(12) Å. The inorganic layered network is stacked along the *c* axis via the mellitate linkers (Figure 9). Free water molecules are intercalated between the layers, with hydrogen bond interactions between terminal aquo species bound to neptunium and remaining non-bonded carboxylate groups. In total, 12 distinct water species have been located from the single-crystal XRD analysis.
In the three-dimensional structure of compound **4**, only four of the carboxylate arms of mellitate molecule are linked to the neptunium centers and act as a pyromellitate ligand. Given that fact, the coordination polymer network of **4** could be related to those of neptunium pyromellitates, previously described in literature. But the structural analysis of the compounds $[Na_3NpO_2(btec)]_2\cdot 11H_2O$[59] and $[(NH_4)_3(NpO_2)_5(btec)_2]\cdot 7H_2O$[60] (btec = 1,2,4,5-benzenetetracarboxylate or pyromellitate) shows assemblies, which differ from that of **4**.

With the mellitate linker, the oxidation of Np(IV) to Np(V) is quite unanticipated, while we obtained single crystals of the U(IV)-mellitate complex under the same synthetic condition. These different results observed for the U- and Np-mellitate complexes probably stem from the different redox behavior between U and Np. It is obvious from the resultant Np(V)-mellitate compound that the hydrothermal synthesis of the initial mixture of $AnCl_4$ and mellitic acid results in the oxidation of An(IV) to a higher oxidation state. The standard redox potential between U(IV) and -(V) (as UO_2^+) is lower than that between Np(IV) and –(V) (as NpO_2^+),[89] indicating that U(IV) could be oxidized more easily than Np(IV). However, it is well known that U(V) has a strong tendency to cause disproportionation (i.e. $2UO_2^+ + H^+ \rightarrow U(IV) + UO_2^{2+} + H_2O$), while the disproportionation of Np(V) is insignificant.[89] This suggests that the U(V) species produced during the hydrothermal synthesis would be disproportionated instantly to eventually form U(IV) and –(VI) (as UO_2^{2+}). As a matter of fact, the UV-Vis absorption measurements on the U-mellitate sample after the hydrothermal synthesis (t = 24h in Fig. S5b in SI) reveal the presence of U(VI) species (at 400-450 nm) in the supernatant, supporting this hypothesis. Hence, it is reasonable to consider that the hydrothermal reaction of the UCl_4 and mellitic acid mixture results in the formation of U(IV)-mellitate complex and

additional U(VI) complexes as dissolved species and/or possible amorphous precipitate which would account for the unidentified impurities found on the powder XRD measurement. In this case, the U(IV)-mellitate compound would have a low solubility to be crystallized, while the uranyl(VI)-mellitates would be fairly soluble in our synthetic conditions. On the other hand, the Np(V) species could be stabilised without disproportionation, forming Np(V)-mellitate complexes. For the phthalate system, the UV-Vis spectrum of the U-mellitate sample after the hydrothermal reaction (t = 24h in Fig. S5a in SI) shows a very small amount of U(VI)/U(IV) species in the supernatant, indicating that the majority of the original U(IV) reacts with the phthalic acid to form the compound **1**.

Thermal behavior of compound 1 ($[U_2O_2(H_2O)_2(1,2\text{-bdc})_2]\cdot H_2O$)

The thermogravimetric analysis has been performed only for the uranium phthalate (**1**) compound, which could be obtained as a pure phase. The thermogravimetric curve (under argon atmosphere; Figure S3a) indicates a weight loss event with two steps. The first loss occurring up to 230°C is attributed to the removal of water molecules (attached and free). The chemical formula deduced from single-crystal XRD analysis would give an expected value of 6.1% wt, for (2+1)H_2O per U_2O_2 unit, but the observed weight loss is lower, with an experimental value of 5.2%. This result indicates that the water content should be lower than expected, and in fact would agree well with a stoechiometry of (2+0.5)H_2O per U_2O_2 (calc.: 5.10%). The latter hypothesis is in good agreement with the value of the remaining weight at 1000°C, after the decomposition of the structure together with the degradation of the organic part. Indeed, the observed final remaining weight value is 61.5% (wt), which fits well with the calculated value (61.3% wt) for UO_2, if one considers 0.5H_2O instead of 1H_2O (calc. value 60.7%) as free water molecules intercalated between the organic-inorganic sheets in compound **1**. The occurrence of UO_2 as final residue of the thermal decomposition of **1** is confirmed by X-ray thermodiffraction experiment (under nitrogen atmosphere; Figure S3b). It indicates the growth of Bragg peaks corresponding to UO_2, from 360°C. It is also observed that the structure of the initial compound **1** persists up to 140°C.

Infrared spectroscopy of compounds 1 and 3

The FT-IR spectrum of compound **1** (Figure S3c) at room temperature confirms the presence of water by the presence of various resonances in the 3700-3000 cm^{-1} range (stretching vibrations). In the case of lanthanide-based coordination polymers possessing only coordinated water molecules, the infrared resonance of aquo group leads to a broad band at around 3300 cm^{-1}. Therefore, in case of the compound **1**, the coordinated water molecules are characterized by the broad band centered at 3300 cm^{-1}, whereas the free water molecules shows the resonance at 3607 cm^{-1}. Bending vibrations of water molecules can be also detected by small peaks between 1650 and 1580 cm^{-1}. The connection between carboxylate arms and U(IV) induces specific vibrations ν_{CO} at 1535 and 1389 cm^{-1}, assigned to the asymmetric and symmetric stretching of water molecules, respectively.

The thermal behavior of compound **1** was also followed by infrared, from RT to 200°C (Figure 10). The relative low affinity of water molecules with the structure is confirmed by the disappearance of the bands between 3700 and 3000 cm^{-1} corresponding to the release of

water molecules. At 120°C, this phenomenon coincides with the appearance of a band centered at 930 cm^{-1}, which is split to two independent vibrations at 945 and 913 cm^{-1} at higher temperature. These values are characteristic to the uranyl(VI) vibrations indicating the oxidation of U(IV) during the heating process and the decomposition of the initial compound.
Due to the presence of impurities in the compound **3**, we selected a few crystals of this phase for the IR characterization. The acquired spectrum is shown in Figure S4. Similar to the compound **1**, coordinated water molecules in **3** generates a large IR band centered at around 3200 cm^{-1}, hiding the resonances coming from the hydroxyl group. In this structure the various connections modes between carboxylate function and uranium involves several resonances in the 1700-900 cm^{-1} range corresponding to stretching vibration ν_{CO}.

Conclusion

The reactivity of aromatic poly-carboxylic acids, phthalic and mellitic acids, with tetravalent uranium and neptunium has been investigated in aqueous media under moderate hydrothermal conditions. Three types of coordination polymers have been revealed: two of them exhibit a similar two-dimensional network with uranium or neptunium. This type of compounds is composed of the connection of square anti-prismatic polyhedral units (AnO_8) via edge sharing mode (with μ_3-oxo bridges) to create infinite zig-zag chains, further being linked to each other via the phthalate molecules. One U(IV) compound with a mellitate ligand has been isolated. Its crystal structure consists of dinuclear $\{U_2O_{10}(OH)_2(H_2O)_2\}$ units (with μ_2-hydroxo bridges) connected by the hexadendate mellitate molecules, forming a dense three-dimensional framework. On the other hand, the reaction of mellitate ligands with Np(IV) in the same synthetic conditions resulted in the formation of a layer-like subnetwork of neptunyl(V) units with a square topology of NpO_2^+, being linked to each other via cation-cation interactions. This eventually results in the formation a three-dimensional structure with the mellitate acting as a linker between the inorganic NpO_2^+-based sheets. These compounds are rare examples of An(IV) coordination polymers produced from aqueous media. Future works will explore the reaction of other polydendate carboxylates with tetravalent actinides in aqueous media.

Acknowledgments

The authors would like to thank Mrs. Nora Djelal & Laurence Burylo, Mr Philippe Devaux for their technical assistances with the SEM images, TG measurements and powder XRD (UCCS). The Chevreul Institute (FR 2638), "Fonds Européen de Développement Régional (FEDER)", "CNRS", "Région Nord Pas-de-Calais" and "Ministère de l'Education Nationale de l'Enseignement Supérieur et de la Recherche" are acknowledged for funding of X-ray diffractometers. The authors also thank TALISMAN for financial support (Project No. TALI_C05-18).

Supporting Information

The supporting Information is available free of charge on the ACS Publications website at DOI: 10.1021/acs.inorg-chem.???. Optical and SEM photographs of **1** and **3**, Optical photographs of **2** and **4**, powder X-ray diffraction patterns of **1**-**4**, thermogravimetric curve of **1**, thermodiffraction diagram of **1**, infrared spectra of **1** and **3**, UV-Vis spectrum of **1**, crystallographic data for **1**, **2**, **3** and **4** (cif files). UV-Vis spectra of the supernatant of **1** and **3**.

Table 1. Crystal data and structure refinements for the obtained uranium/neptunium carboxylates.

	1	**2**	**3**	**4**
Formula	$C_{16}H_{12}O_{13}U_2$	$C_{16}H_{12}O_{13}Np_2$	$C_{12}H_4O_{16}U_2$	$C_{24}O_{70}Np_{10}$
Formula weight	888.32	886.26	880.21	3778.7
Temperature/K	300	100	300	100
Crystal type	green plate	brown plate	green block	green plate
Crystal size/mm	0.14 x 0.06 x 0.06	0.13 x 0.06 x 0.06	0.09 x 0.07 x 0.06	0.17 x 0.10 x 0.03
Crystal system	triclinic	triclinic	orthorhombic	monoclinic
Space group	*P*-1	*P*-1	*Fdd*2	*Pn*
a/Å	7.8178(7)	7.7880(8)	13.903(3)	12.9650(3)
b/Å	9.5870(9)	9.4753(10)	19.813(5)	12.9796(3)
c/Å	13.2310(13)	13.1220(14)	11.393(3)	20.1038(5)
α/°	77.492(6)	77.747(3)	90	90
β/°	86.775(5)	86.824(3)	90	95.1696(5)
γ°	83.487(5)	83.448(3)	90	90
Volume/Å^3	961.36(16)	939.60(17)	3138.4(14)	3369.32(14)
Z, $\rho_{calculated}$/g.cm^{-3}	2, 3.069	2, 3.062	8, 3.726	2, 3.725
μ/mm^{-1}	16.896	10.821	20.714	15.407
Θ range/°	1.58 – 26.39	2.63 – 26.40	2.53 – 26.45	2.22 – 26.67
Limiting indices	$-9 \le h \le 9$ $-11 \le k \le 11$ $-16 \le l \le 16$	$-9 \le h \le 9$ $-11 \le k \le 11$ $-16 \le l \le 16$	$-17 \le h \le 17$ $-24 \le k \le 23$ $-14 \le l \le 14$	$-16 \le h \le 14$ $-16 \le k \le 16$ $-25 \le l \le 25$
Collected reflections	24286	61364	13003	78412
Unique reflections	3929 [R(int) = 0.0581]	3862 [R(int) = 0.0587]	1589 [R(int) = 0.0907]	63506 [R(int) = 0.1871]
Parameters	282	257	131	467
Goodness-of-fit on F^2	1.03	1.02	1.02	1.08
Final R indices [I>2σ(I)]	R1 = 0.0253 wR2 = 0.0481	R1 = 0.0217 wR2 = 0.0393	R1 = 0.0477 wR2 = 0.0995	R1 = 0.0352 wR2 = 0.0372
R indices (all data)	R1 = 0.0395 wR2 = 0.0529	R1 = 0.0344 wR2 = 0.0418	R1 = 0.0707 wR2 = 0.1078	R1 = 0.0390 wR2 = 0.0486
Largest diff. peak and hole/e.Å^{-3}	1.13 and -1.03	1.02 and -0.98	2.86 and -1.72	1.50 and -1.84

References

(1) Loiseau, T.; Mihalcea, I.; Henry, N.; Volkringer, C. *Coord. Chem. Rev.* **2014**, *266-267*, 69.

(2) Wang, K.-X.; Chen, J. S. *Acc. Chem. Res.* **2011**, *44*, 531.

(3) Andrews, M. B.; Cahill, C. L. *Chem. Rev.* **2013**, *113*, 1121.

(4) Takao, S.; Takao, K.; Kraus, W.; Emmerling, F.; Scheinost, A. C.; Bernhard, G.; Hennig, C. *Eur. J. Inorg. Chem.* **2009**, 4771.

(5) Knope, K. E.; Wilson, R. E.; Vasiliu, M.; Dixon, D. A.; Soderholm, L. *Inorg. Chem.* **2011**, *50*, 9696.

(6) Vasiliu, M.; Knope, K. E.; Soderholm, L.; Dixon, D. A. *J. phys. Chem. A* **2012**, *116*, 6917.

(7) Hu, Y.-J.; Knope, K. E.; Skanthakumar, S.; Soderholm, L. *Eur. J. Inorg. Chem.* **2013**, 4159.

(8) Hennig, C.; Takao, S.; Takao, K.; Weiss, S.; Kraus, W.; Emmerling, F.; Scheinost, A. C. *Dalton Trans.* **2012**, *41*, 12818.

(9) Falaise, C.; Charles, J. S.; Volkringer, C.; Loiseau, T. *Inorg. Chem.* **2015**, *54*, 2235.

(10) Nocton, G.; Burdet, F.; Pécaut, J.; Mazzanti, M. *Angew. Chem., Int. Ed.* **2007**, *46*, 7574.

(11) Mougel, V.; Biswas, B.; Pécaut, J.; Mazzanti, M. *Chem. Commun.* **2010**, *46*, 8648.

(12) Falaise, C.; Volkringer, C.; Vigier, J.-F.; Henry, N.; Beaurain, A.; Loiseau, T. *Chem. Eur. J.* **2013**, *19*, 5324.

(13) Falaise, C.; Volkringer, C.; Férey, G. *Cryst. Growth Des.* **2013**, *13*, 3225.

(14) Falaise, C.; Assen, A.; Mihalcea, I.; Volkringer, C.; Mesbah, A.; Dacheux, N.; Loiseau, T. *Dalton Trans.* **2015**, *44*, 2639.

(15) Knope, K. E.; Soderholm, L. *Inorg. Chem.* **2013**, *52*, 6770.

(16) Tamain, C.; Dumas, T.; Guillaumont, D.; Hennig, C.; Guilbaud, P. *Eur. J. Inorg. Chem.* **2016**, 3536.

(17) Toledano, P.; Ribot, F.; Sanchez, C. *C.R. Acad. Sci. Paris, Ser. II* **1990**, *311*, 1315.

(18) Mereacre, V.; A.M., A.; Akhtar, M. N.; Lindemann, A.; Anson, C. E.; Powell, A. K. *Helv. Chim. Acta* **2009**, *92*, 2507.

(19) Das, R.; Sarma, R.; Baruah, J. B. *Inorg. Chem. Commun.* **2010**, *13*, 793.

(20) Hennig, C.; Ikeda-Ohno, A.; Kraus, W.; Weiss, S.; Pattison, P.; Emerich, H.; Abdala, P. M.; Scheinost, A. C. *Inorg. Chem.* **2013**, *52*, 11734.

(21) Estes, S. L.; Antonio, M. R.; Soderholm, L. *J. Phys. Chem. C* **2016**, *120*, 5810.

(22) Falaise, C.; Volkringer, C.; Vigier, J.-F.; Beaurain, A.; Roussel, P.; Rabu, P.; Loiseau, T. *J. Am. Chem. Soc.* **2013**, *135*, 15678.

(23) Biswas, B.; Mougel, V.; Pécaut, J.; Mazzanti, M. *Angew. Chem., Int. Ed.* **2011**, *50*, 5745.

(24) Falaise, C.; Delille, J.; Volkringer, C.; Loiseau, T. *Eur. J. Inorg. Chem.* **2015**, 2813.

(25) Volkringer, C.; Mihalcea, I.; Vigier, J.-F.; Beaurain, A.; Visseaux, M.; Loiseau, T. *Inorg. Chem.* **2011**, *50*, 11865.

(26) Martin, N. P.; Volkringer, C.; Falaise, C.; Henry, N.; Loiseau, T. *Cryst. Growth Des.* **2016**, *16*, 1667.

(27) Falaise, C.; Volkringer, C.; Loiseau, T. *Inorg. Chem. Commun.* **2014**, *39*, 26.
(28) Zhang, Y.; Kadi, F.; Karatchevtseva, I.; Price, J. R.; Murphy, T.; Wuhrer, R.; Li, F.; Lumpkin, G. R. *J. Incl. Phenom. Macrocyl. Chem.* **2015**, *82*, 163.
(29) Ok, K. M.; Sung, J.; Hu, G.; Jacobs, R. M. J.; O'Hare, D. *J. Am. Chem. Soc.* **2008**, *130*, 3762.
(30) Kim, J. Y.; Norquist, A. J.; O'Hare, D. *J. Am. Chem. Soc.* **2003**, *125*, 12688.
(31) Ok, K. M.; O'Hare, D. *Dalton Trans.* **2008**, 5560.
(32) Frisch, M.; Cahill, C. L. *Cryst. Growth Des.* **2008**, *8*, 2921.
(33) Ziegelruber, K. L.; Knope, K. E.; Frisch, M.; Cahill, C. L. *J. Solid State Chem.* **2008**, *181*, 373.
(34) Thuéry, P. *Inorg. Chem.* **2011**, *50*, 1898.
(35) Li, Y.; Weng, Z.; Wang, Y.; Chen, L.; Sheng, D.; Diwu, J.; Chai, Z.; Albrecht-Schmitt, T. E.; Wang, S. *Dalton Trans.* **2016**, *45*, 918.
(36) Li, Y.; Weng, Z.; Wang, Y.; Chen, L.; Sheng, D.; Liu, Y.; Diwu, J.; Chai, Z.; Albrecht-Schmitt, T. E.; Wang, S. *Dalton Trans.* **2015**, *44*, 20867.
(37) Knope, K. E.; Soderholm, L. *Chem. Rev.* **2013**, *113*, 944.
(38) Neck, V.; Kim, J. I. *Radiochim. Acta* **2001**, *89*, 1.
(39) Walther, C.; Deneke, M. A. *Chem. Rev.* **2013**, *113*, 995.
(40) Duvieubourg-Garela, L.; Vigier, N.; Abraham, F.; Grandjean, S. *J. Solid State Chem.* **2008**, *181*, 2008.
(41) Vazquez, G. J.; Dodge, C. J.; Francis, A. J. *Inorg. Chem.* **2009**, *48*, 9485.
(42) Robl, C.; Kuhs, W. F. *J. Solid State Chem.* **1991**, *92*, 101.
(43) Husar, R.; Hübner, R.; Hennig, C.; Martin, P. M.; Chollet, M.; Weiss, S.; Stumpf, T.; Zänker, H.; Ikeda-Ohno, A. *Chem. Comm.* **2015**, *51*, 1301.
(44) Kaszuba, J. P.; Runde, W. H. *Environ. Sci. Technol.* **1999**, *33*, 4427.
(45) Hauck, J. *Inorg. Nucl. Chem. Lett.* **1976**, *12*, 617.
(46) Charushnikova, I. A.; Krot, N. N.; Makarenkov, V. I. *Radiochem.* **2015**, *57*, 233.
(47) Charushnikova, I. A.; Krot, N. N.; Starikova, Z. A. *Radiochim. Acta* **2009**, *97*, 587.
(48) Charushnikova, I. A.; Krot, N. N.; Starikova, Z. A. *Radiochim. Acta* **2007**, *95*, 495.
(49) Budantseva, N. A.; Andreev, G. B.; Fedoseev, A. M.; Antipin, M. Y.; Krupa, J. C. *Radiochim. Acta* **2006**, *94*, 69.
(50) Charushnikova, I. A.; Budantseva, N. A.; Fedoseev, A. M. *Radiochem.* **2015**, *57*, 240.
(51) Grigoriev, M. S.; Charushnikova, I. A.; Fedoseev, A. M. *Radiochem.* **2015**, *57*, 386.
(52) Charushnikova, I. A.; Grigoriev, M. S.; Krot, N. N. *Radiochim. Acta* **2011**, *99*, 197.
(53) Andreev, G. B.; Antipin, M. Y.; Budantseva, N. A.; Krot, N. N. *Russ. J. Coord. Chem.* **2005**, *31*, 800.
(54) Grigoriev, M. S.; Krot, N. N.; Bessonov, A. A.; Suponitsky, K. Y. *Acta Cryst. E* **2007**, *63*, m561.
(55) Charushnikova, I. A.; Krot, N. N.; Starikova, Z. A. *Radiochem.* **2001**, *43*, 496.
(56) Yusov, A. B.; Charushnikova, I. A.; Fedoseev, A. M.; Bessonov, A. A. *Radiochem.* **2014**, *56*, 134.
(57) Charushnikova, I. A.; Krot, N. N.; Grigoriev, M. S. *Radiochem.* **2014**, *56*, 468.
(58) Cousson, A.; Dabos, S.; Abazli, H.; Nectoux, F.; Pages, M. *J. Less Common Metals* **1984**, *99*, 233.

(59) Nectoux, F.; Abazli, H.; Jové, J.; Cousson, A.; Gasperin, M.; Choppin, G. *J. Less Common Metals* **1984**, *97*, 1.
(60) Cousson, A. *Acta Cryst. C* **1985**, *41*, 1758.
(61) Charushnikova, I. A.; Krot, N. N.; Starikova, Z. A. *Radiochem.* **2001**, *43*, 492.
(62) Tian, G.; Rao, L.; Teat, S. J. *Inorg. Chem.* **2009**, *48*, 10158.
(63) Grigoriev, M. S.; Antipin, M. Y.; Krot, N. N.; Bessonov, A. A. *Radiochim. Acta* **2004**, *92*, 405.
(64) Charushnikova, I. A.; Grigoriev, M. S.; Krot, N. N. *Radiochem.* **2010**, *52*, 138.
(65) Sokolova, M. N.; Bessonov, A. A.; Fedoseev, A. M. *Radiochem.* **2012**, *54*, 341.
(66) Charushnikova, I. A.; Krot, N. N.; Makarenkov, V. I. *Inorg. Chem.* **2010**, *49*, 7611.
(67) Yusov, A. B.; Mishkevich, V. I.; Fedoseev, A. M.; Grigoriev, M. S. *Radiochem.* **2013**, *55*, 269.
(68) *SAINT Plus Version 7.53a, Bruker Analytical X-ray Systems, Madison, WI* **2008**.
(69) Sheldrick, G. M. *SADABS, Bruker-Siemens Area Detector Absorption and Other Correction, Version 2008/1* **2008**.
(70) Sheldrick, G. M. *Acta Cryst. A* **2008**, *64*, 112.
(71) Petricek, V.; Dusek, M.; Palatinus, L. *Z. Kristallogr.* **2014**, *229*, 345.
(72) Morss, L. R.; Edelstein, N. M.; Fuger, J.; Katz, J. J. *The Chemistry of the Actinide and Transactinide Elements (Set Vol.1-6), Springer Netherlands* **2011**.
(73) Brese, N. E.; O'Keeffe, M. *Acta Crystallogr. B* **1991**, *47*, 192.
(74) Desgranges, L.; Baldinozzi, G.; Rousseau, G.; Nièpce, J.-C.; Calvarin, G. *Inorg. Chem.* **2009**, *48*, 7585.
(75) Lander, G. H.; Mueller, M. H. *Phys. Rev. B* **1974**, *10*, 1994.
(76) Jelenic, I.; Grdenic, D.; Bezjak, A. *Acta Cryst.* **1964**, *17*, 758.
(77) Lundgren, G. *Arkiv Kem.* **1952**, *4*, 421.
(78) Hashem, E.; Swinburne, A. N.; Schulzke, C.; Evans, R. C.; Platts, J. A.; Kerridge, A.; Natrajan, L. S.; Baker, R. J. *RSC Advances* **2013**, *3*, 4350.
(79) Le Borgne, T.; Thuery, P.; Ephritikhine, M. *Acta Cryst. C* **2002**, *58*, m8.
(80) Jin, G. B.; Skanthakumar, S.; Soderholm, L. *Inorg. Chem.* **2011**, *50*, 5203.
(81) Forbes, T. Z.; Burns, P. C. *J. Solid State Chem.* **2009**, *182*, 43.
(82) Jin, G. B.; Skanthakumar, S.; Soderholm, L. *Inorg. Chem.* **2012**, *51*, 3220.
(83) Jin, G. B.; Skanthakumar, S.; Soderholm, L. *Inorg. Chem.* **2011**, *50*, 6297.
(84) Krot, N. N.; Grigoriev, M. S. *Russ. Chem. Rev.* **2004**, *73*, 89.
(85) Albrecht-Schmitt, T. E.; Almond, P. M.; Sykora, R. E. *Inorg. Chem.* **2003**, *42*, 3788.
(86) Wang, S.; Alekseev, E. V.; Miller, H. M.; Depmeier, W.; Albrecht-Schmitt, T. E. *Inorg. Chem.* **2010**, *49*, 9755.
(87) Grigoriev, M. S.; Bessonov, A. A.; Krot, N. N.; Yanovskii, A. I. *Radiochem.* **1993**, *35*, 382.
(88) Grigoriev, M. S.; Charushnikova, I. A.; Krot, N. N.; Yanovskii, A. I.; Struchkov, Y. T. *Radiochem.* **1993**, *35*, 394.
(89) Kihara, S.; Yoshida, Z.; Aoyagi, H.; Maeda, K.; Shirai, O.; Kitatsuji, Y.; Yoshida, Y. *Pure Appl. Chem.* **1999**, *71*, 1771.

Figures

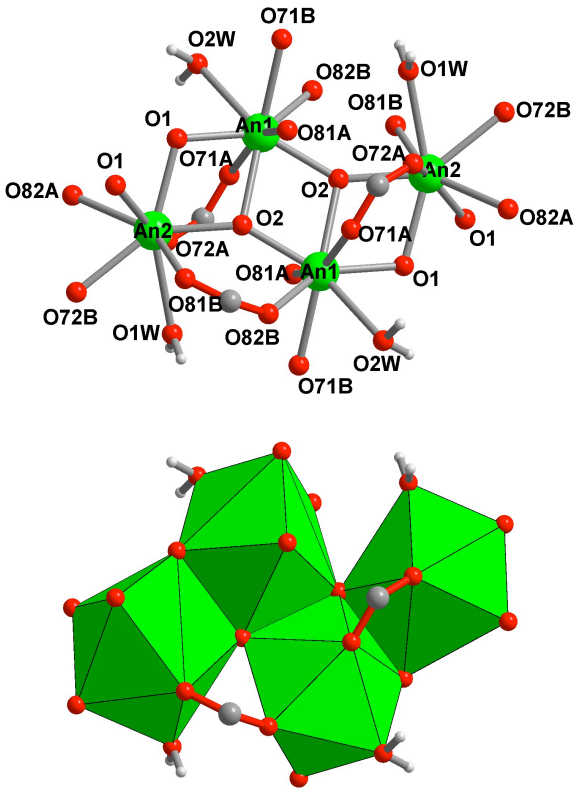

Figure 1: Coordination environments around the two types of actinides centers in $[An_2O_2(H_2O)_2(1,2\text{-bdc})_2]\cdot H_2O$ (An = U^{4+} (**1**), Np^{4+} (**2**)). O1 and O2 are μ_3-oxo groups, shared between three neighboring actinide cations. OW1 and OW2 are aquo species in terminal positions. Green circles: uranium or neptunium; red circles: oxygen; grey circles: carbon; light grey circles: hydrogen.

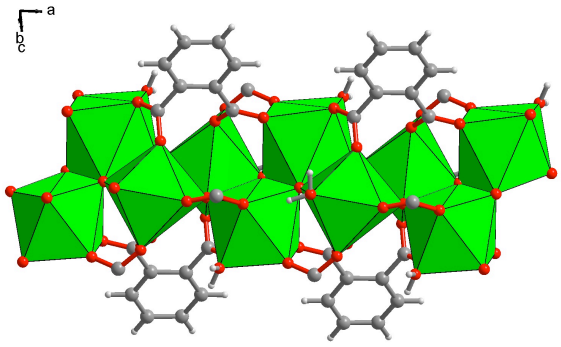

Figure 2: Views of the infinite ribbons of square antiprismatic units AnO_8, sharing edge, and developing along the *a* axis, in $[An_2O_2(H_2O)_2(1,2\text{-bdc})_2]\cdot H_2O$ (An = U^{4+} (**1**), Np^{4+} (**2**)). The connection mode of one type of phthalate ligand is shown within the chain.

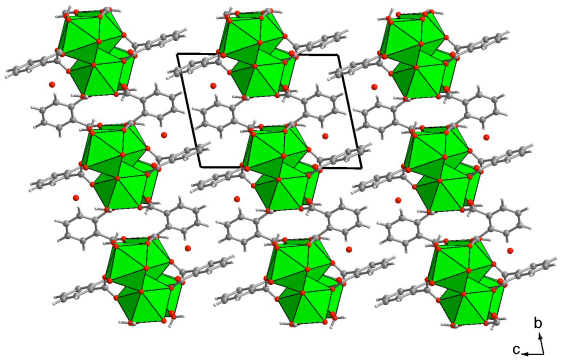

Figure 3: Crystal structure of $[An_2O_2(H_2O)_2(1,2\text{-bdc})_2]\cdot H_2O$ (An = U^{4+} (**1**), Np^{4+} (**2**)), in the (*b*,*c*) plane. Isolated red circle indicate the free water molecules (O3W) intercalated between the inorganic chains.

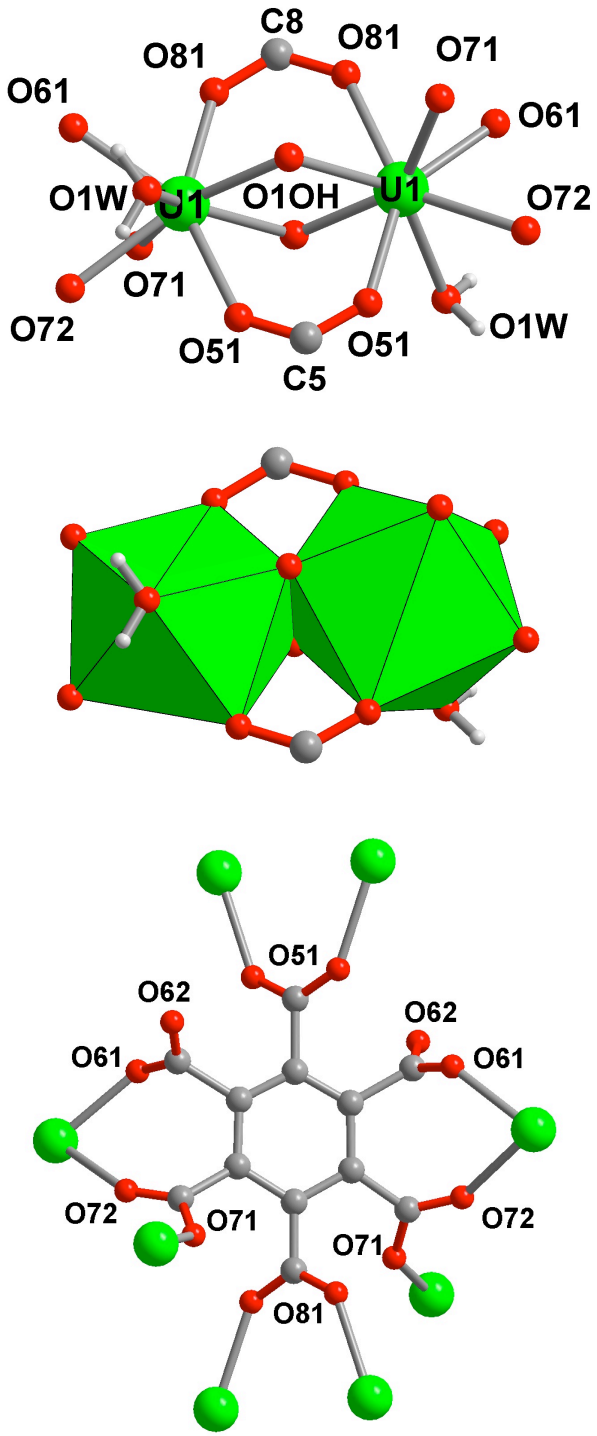

Figure 4: (top) Coordination modes of the eight-fold uranium center (U1) in compound **3** ($U_2(OH)_2(H_2O)_2$(mel)), defined in an dinuclear unit $\{U_2O_{10}(OH)_2(H_2O)_2\}$. The uranium atoms are connected through two μ_2-OH groups. (bottom) Coordination mode of mellitate ligand. Green circles: uranium; red circles: oxygen; grey circles: carbon; light grey circles: hydrogen.

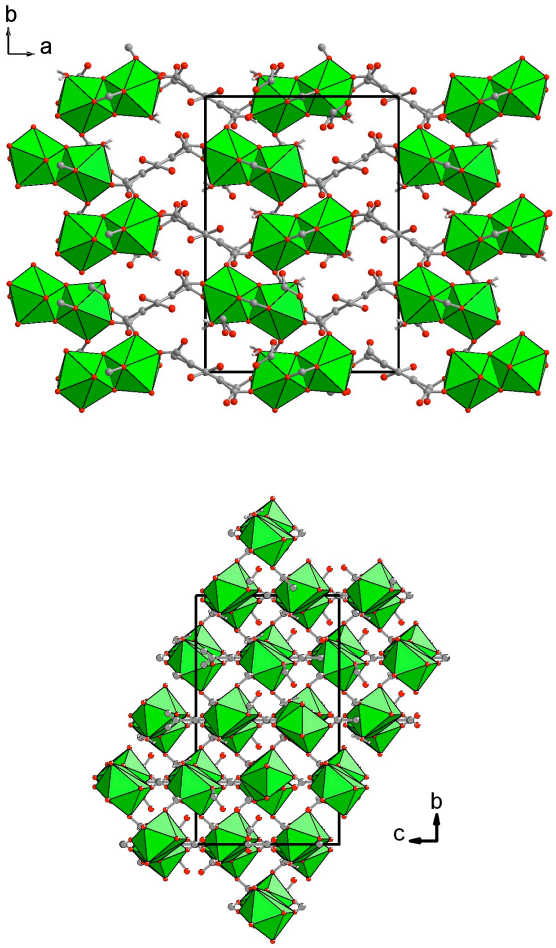

Figure 5: (top) Crystal structure of compound **3** ($U_2(OH)_2(H_2O)_2$(mel)) in the (*a*,*b*) plane, showing the connection of the dinuclear units $\{U_2O_{10}(OH)_2(H_2O)_2\}$ with the mellitate ligands. (bottom) View of the structure of **3** in the (*b*,*c*) plane, indicating the stacking the of (*a*,*b*) organic-inorganic sub-layers along the [011] direction.

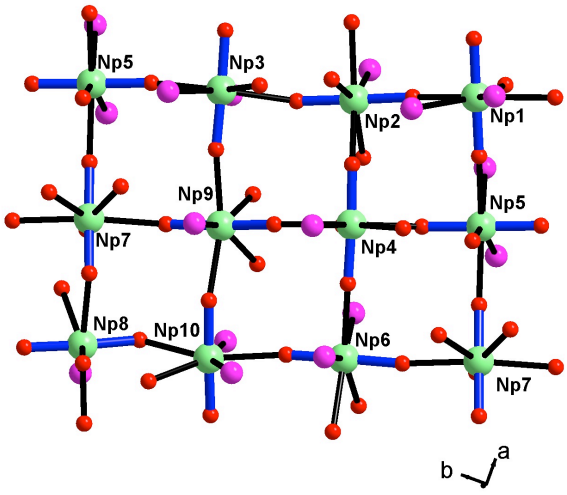

Figure 6: View of the asymmetric unit of $[(NpO_2)_{10}(H_2O)_{14}(Hmel)_2]\cdot 12H_2O$ (**4**) showing the connection mode of the ten crystallographically independent neptunium centers linked to each other through 'yl' oxo groups, corresponding the cation-cation interaction (CCI). Green circles: neptunium atoms; red circle: oxygen atoms; purple circles: terminal water molecules. blue bonds: neptunyl bond (Np=O); black bonds: Np-O.

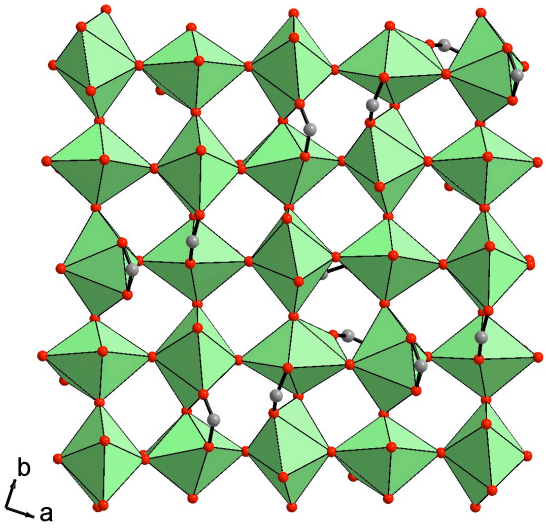

Figure 7: Polyhedral representation of the inorganic sheet in $([(NpO_2)_{10}(H_2O)_{14}(Hmel)_2]\cdot 12H_2O)$ (**4**), showing the cation-cation interaction linkage of the $\{NpO_7\}$ polyhedra, in a square net.

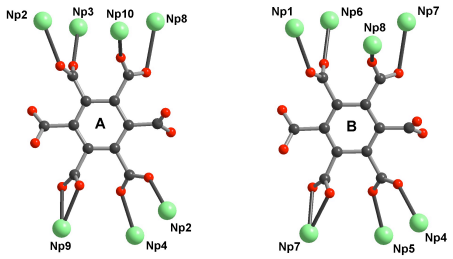

Figure 8: Coordination modes of the two distinct mellitate ligands (labeled A & B) in compound **4**.

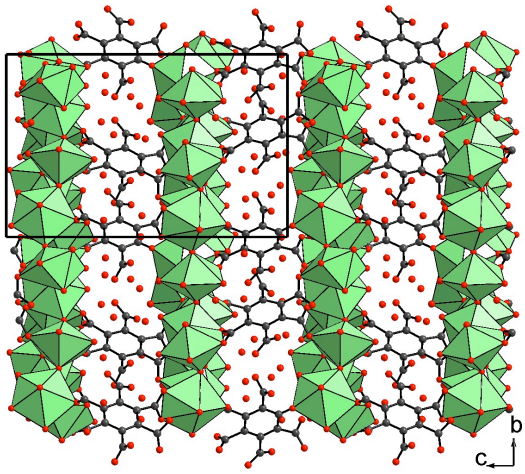

Figure 9: Crystal structure of $[(NpO_2)_{10}(H_2O)_{14}(Hmel)_2]\cdot 12H_2O$ (**4**) in the (*b*,*c*) plane showing the stacking of the square layered net along the *c* axis. Isolated red circles represent the free water molecules, intercalated between the inorganic sheets.

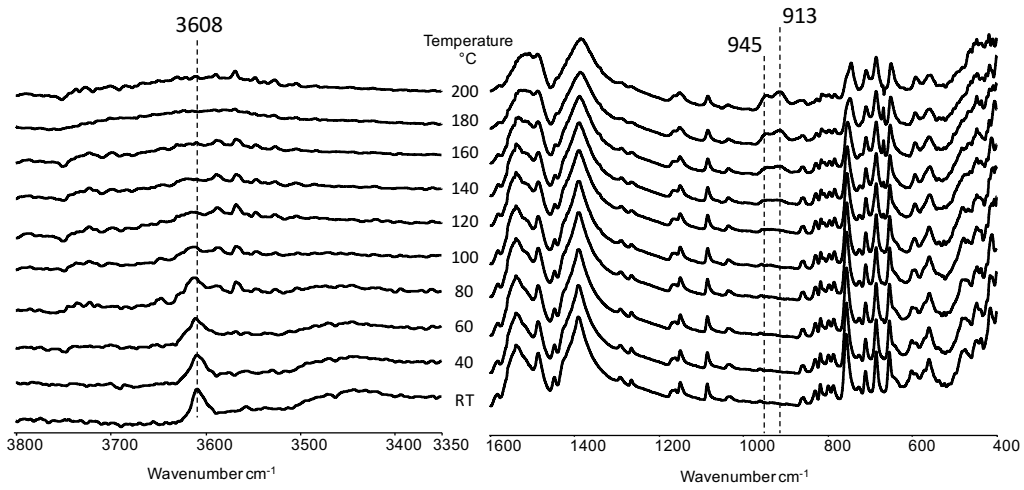

Figure 10: In situ infrared spectra of compound **1** between 20 and 200°C, with the selected ranges of 3800-3350 cm^{-1} and 1600-400 cm^{-1}.